Square Arrays of Holes and Dots Patterned from a Linear ABC Triblock Terpolymer

Hong Kyoon Choi,[†] Jessica Gwyther,[‡] Ian Manners,[‡] and Caroline A. Ross[†,*]

[†]Department of Materials Science and Engineering, Massachusetts Institute of Technology, Cambridge, Massachusetts 02139, United States and [‡]School of Chemistry, University of Bristol, Bristol BS8 ITS, U.K.

ABSTRACT

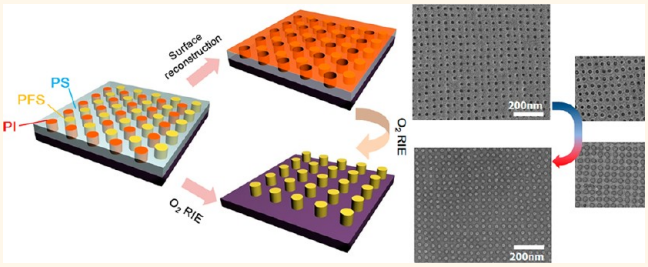

Microphase separation of a polyisoprene-*b*-polystyrene-*b*-polyferrocenylsilane (PI-*b*-PS-*b*-PFS) triblock terpolymer film during chloroform solvent-annealing formed a 44 nm period square-symmetry array of alternating PI and PFS cylinders in a PS matrix. This nanostructure was converted to either a positive pattern of posts or a negative pattern of holes with tunable diameter by oxygen reactive ion etching or by surface reconstruction in a solvent, respectively, and coexisting post and hole patterns were also formed. Square arrays of silicon posts, pits, and inverted pyramids were fabricated by pattern transfer from the triblock terpolymer film into silicon substrates. The morphology of the triblock terpolymer film varied with the chloroform vapor pressure during solvent annealing, which was explained by selective swelling of the PI block at high vapor pressures. This triblock terpolymer system provides a convenient block copolymer lithography process for generation of nanoscale posts or holes with square symmetry.

KEYWORDS: block copolymer · triblock terpolymer · self-assembly · nanolithography · square pattern · solvent vapor annealing

Microphase-separated periodic structures of block copolymers have been studied widely because they offer a simple and low-cost nanopatterning methodology. In particular, thin films of block copolymers can be used as nanolithography masks for fabrication of devices.[1−9] Although there are many types of block copolymers, AB diblock copolymers have received most attention both experimentally and theoretically due to their relative simplicity and their ability to form either line-space patterns or close-packed dot or hole patterns. A wider range of self-assembled morphologies can be obtained from ABC triblock terpolymers,[10−12] and this has stimulated research into their thin-film behavior.[13−16] An AB diblock copolymer can be modeled using two parameters, $\chi_{AB}N$ and f_A, which specify the equilibrium morphology (where χ is the Flory−Huggins parameter, N the degree of polymerization, and f_A the A-block volume fraction), but an ABC triblock terpolymer requires three interaction parameters (χ_{AB}, χ_{BC}, χ_{AC}), two independent volume fractions (f_A, f_B, with $f_C = 1 - f_A - f_B$), and a definition of the block sequence, such as linear or a miktoarm star architecture.[10−12] Because of the large number of parameters, triblock terpolymers can self-assemble into dozens of fascinating periodic structures,[10−12,17−25] while an AB diblock copolymer can form a more limited set of morphologies including lamellar, cylindrical, spherical, and gyroid.[26−28]

A particularly interesting structure from the point of view of microelectronic device fabrication is the square-symmetry array, which can be formed spontaneously by an ABC linear triblock terpolymer with specific ranges of volume fractions and interaction parameters,[10,17,29−32] where $\chi_{AC} > \chi_{AB}$ and χ_{BC} and $f_B = 0.6−0.7$. In the bulk ABC linear triblock terpolymer, cylinders of A and C form an alternating checkerboard pattern in a matrix of the majority B block. Square-symmetry structures can also be formed from a blend of diblock copolymers that form hydrogen bonds, mimicking an ABC linear triblock terpolymer;[33] or from templating of diblock copolymer films by a patterned substrate.[34,35] In a previous study, we obtained square-symmetry microdomains from an ABC linear triblock terpolymer thin film of polyisoprene-*b*-polystyrene-*b*-polyferrocenylsilane (PI-*b*-PS-*b*-PFS) blended with PS homopolymer.[30,31] Etching the film in oxygen reactive ion etch (RIE) removed the PI and PS, leaving oxidized PFS posts in a square

* Address correspondence to caross@mit.edu.

Received for review July 10, 2012 and accepted August 21, 2012.

Published online August 21, 2012
10.1021/nn303085k

array. The quality of ordering (correlation length) was increased by using a nonpreferential brush layer on the substrate such as polyethylene oxide (PEO) or poly(2-vinylpyridine) (P2VP) that was chemically dissimilar to all three blocks.[30] The nonpreferential brush layer promoted a vertical cylinder orientation in which all three blocks contacted the substrate, in contrast to a preferential brush layer, which induced formation of a wetting layer and led to spherical PI and PFS microdomains.

Microphase separation of the triblock terpolymer film can be accomplished by thermal annealing below the order−disorder temperature or by annealing in a solvent vapor, usually at room temperature. The vapor pressure and selectivity of the solvent(s) used during solvent vapor annealing lead to different degrees of swelling of the blocks and consequently control over the morphology of the film. Russell *et al*., Kramer *et al*.,[29,36] and our earlier work used solvent vapor to anneal triblock terpolymers,[21,30,31] and Krausch *et al*.[37] and Han *et al*.[38] demonstrated the effects of solvent type and annealing time on triblock terpolymer morphology. Despite this, there has not been a study of the effect of vapor pressure on triblock terpolymer morphology. In addition, research to date has mainly focused on pattern formation from only one of the three blocks (*e.g*., making posts from PFS by removing the other two blocks),[30] but this approach does not take full advantage of the three different block chemistries that are available. Hillmyer *et al*. proposed the use of more than one etching process in a triblock terpolymer system,[39] and Hawker *et al*. demonstrated different nanoscale patterns by applying two orthogonal etching processes to a blend of diblock copolymers.[40] In this work, we show that the three blocks in a PI-*b*-PS-*b*-PFS triblock copolymer can not only form various morphologies using a continuous-flow solvent annealing system but also provide routes to generate patterns consisting of posts, holes, or a combination. Pattern transfer from the hole/post patterns is demonstrated *via* dry etching and anisotropic wet etching.

RESULTS AND DISCUSSION

An 82 kg/mol (M_n) PI-*b*-PS-*b*-PFS triblock terpolymer was used with volume fractions of 25%, 65%, and 10%, respectively, dissolved in toluene at 0.85 wt %. PS homopolymer of molecular weight 27 kg/mol (M_n) was added to the solution at 0.15 wt % to increase the range of film thickness over which the square-symmetry pattern forms.[30,31] Spin-cast films were annealed in flowing chloroform vapor diluted with nitrogen gas. The thin film morphology is shown schematically in Figure 1a. Previously, we have shown that the self-assembled microdomain structure of PI-*b*-PS-*b*-PFS can be processed to form PFS posts by removing the PI and PS simultaneously, relying on the higher etching resistance of the silicon- and iron-containing PFS phase in oxygen RIE.[30,31] In this study, we combined

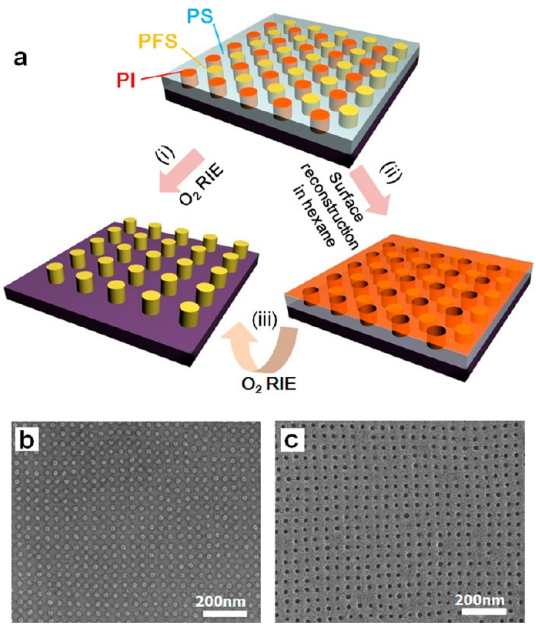

Figure 1. (a) Schematic illustration of the self-assembled structure of the PI-*b*-PS-*b*-PFS triblock terpolymer thin film, and pattern developing processes (i) to form a square array of posts and (ii) a square array of holes and (iii) from holes to posts. SEM images of (b) PFS post pattern after oxygen RIE and (c) hole pattern after surface reconstruction.

the oxygen RIE process (Figures 1a (i) and 1b) with a second process that formed a square array of holes by surface reconstruction of the PI as described in Figure 1a (ii). Surface reconstruction is a convenient way to generate holes from a cylinder morphology block copolymer film.[41,42] Immersing the self-assembled PI-*b*-PS-*b*-PFS triblock terpolymer film in liquid hexane, which is a good solvent for PI and a poor solvent for PS and PFS, swelled the PI block, which diffused to cover the top surface of the film. A rapid quench of the solvent concentration with nitrogen gas shrank the PI and generated holes where the PI cylinders had been located, leaving the PI on the film surface. Figure 1c is an SEM image of a square array of holes produced by surface reconstruction in hexane. The average diameter of the holes was 15 nm and the pitch was 44 nm. The PFS microdomains were still present as a square array within the film even after surface reconstruction. Therefore an additional oxygen RIE step could transform the hole pattern to a post pattern as described (Figure 1a (iii)) by removing the PI and PS. The oxygen RIE widened the holes left by the PI, which then merged to leave the PFS as posts, as shown in Figure 2. The average diameter of holes just after surface reconstruction was 15 nm (Figure 2a) and was widened to 21 nm (Figure 2b) and 30 nm (Figure 2c) by oxygen RIE for 10 or 15 s, respectively. After 30 s the PS and remaining PI were removed, to form a PFS post array (Figure 2d). We also demonstrated a mixed morphology consisting of holes and posts by applying these two processes in sequence, described in Figure 2e.

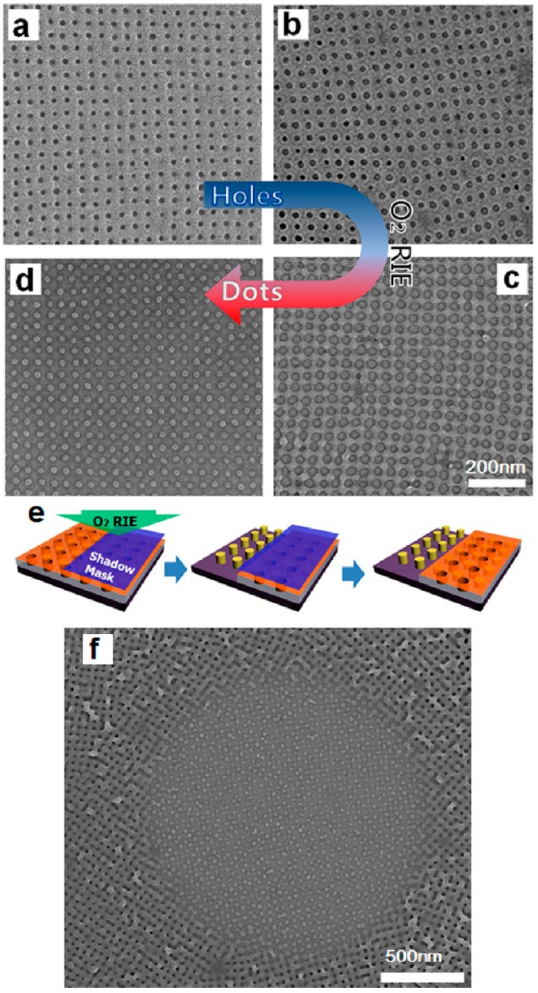

Figure 2. SEM images of PI-*b*-PS-*b*-PFS triblock terpolymer thin films (a) just after surface reconstruction, (b) after an additional oxygen RIE for 10 s, (c) after additional RIE for 15 s, and (d) after additional RIE for 30 s. The average diameter of holes increased from (a) 15 nm to (b) 21 nm and (c) 30 nm, and (d) holes merged to leave posts. (e) Schematic process for mixed morphology holes and posts and (f) corresponding SEM image. Scale bar in (a, b, c, d) is the same.

First, a hole pattern was generated by surface reconstruction in hexane; then a region of the film was transformed to a post pattern by oxygen RIE using a 1.2 μm diameter holey carbon film as a shadow mask, Figure 2f.

Figure 3 shows the transfer of these morphologies into a silicon substrate. A pattern of posts was etched into the substrate by CF_4 RIE (Figure 3a) using the array of PFS posts formed from oxygen-etching the triblock terpolymer film as a mask. A similar process was applied to transfer a hole pattern, Figure 3b. A 5 s oxygen RIE was employed to remove the polymer brush layer at the bottom of holes before etching the substrate by CF_4 RIE followed by oxygen RIE to remove the remaining polymer mask. The average diameter and depth of the transferred holes were 19 and 20 nm, respectively. The diameter of the transferred holes was varied by tuning the initial size of the holes in the triblock terpolymer film by changing the oxygen RIE time.

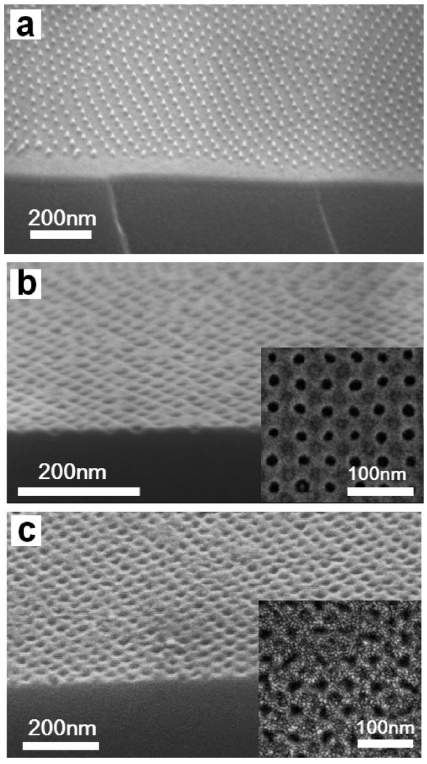

Figure 3. SEM images of transferred patterns on silicon substrates from a PI-*b*-PS-*b*-PFS triblock terpolymer. (a) Square array of silicon posts transferred from PFS post pattern *via* CF_4 RIE. (b) Square array of pits transferred from the polymer hole pattern *via* CF_4 RIE. (c) Array of silicon inverted pyramids transferred from the polymer hole pattern *via* anisotropic KOH wet etching. All the residual polymer was removed after pattern transfer by oxygen RIE.

Pattern transfer using wet chemical etching was also investigated. The silicon was etched anisotropically by a 30% KOH solution for 4 min at room temperature, forming an inverted pyramid structure bounded by (111) planes[43−45] (Figure 3c) from a triblock terpolymer film with widened holes. The facets of the inverted pyramids are hard to resolve, but the plan view inset shows the square shape of the pits in contrast to Figure 3b. The location of the pits can be controlled by templating the triblock terpolymer using topographical features,[30] and this silicon inverted pyramid structure may be useful in studies of physical phenomena such as templated agglomeration.[46]

The sensitivity of the morphology of a triblock terpolymer to small variations in volume fraction of the blocks enables tunability of the structure *via* solvent annealing. In our previous PI-*b*-PS-*b*-PFS triblock copolymer study, a simple solvent annealing system was used in which the sample is placed in a chamber with a leak containing a reservoir of liquid solvent and exposed to a solvent vapor.[30,31] This simple solvent annealing system has poor controllability of solvent vapor pressure; the solvent vapor pressure decreases as the solvent evaporates and escapes from the chamber. To better quantify the effects of vapor pressure, in this work a flow-controlled

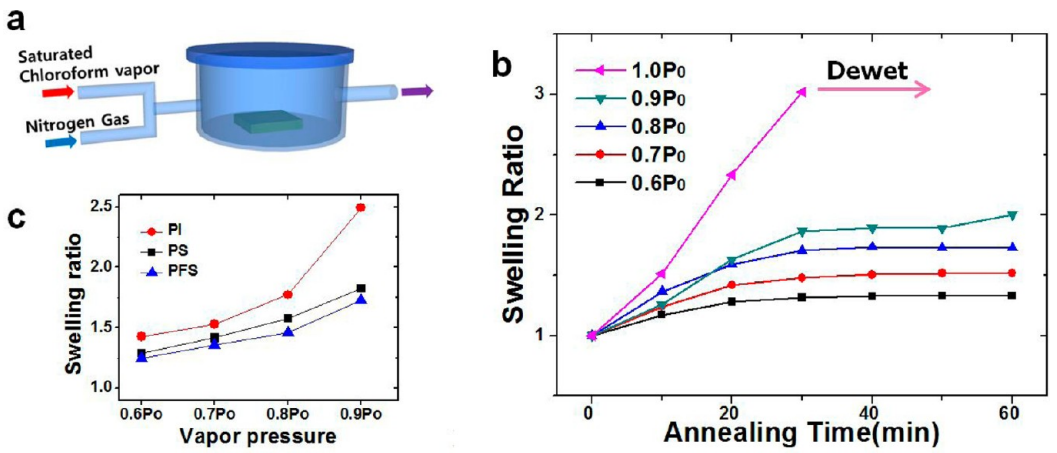

Figure 4. (a) Schematic of flow-controlled solvent vapor annealing system. (b) Change of swelling ratio of PI-*b*-PS-*b*-PFS triblock terpolymer film during solvent annealing at five different chloroform vapor pressures. (c) Plot of saturated swelling ratio of PI, PS, and PFS homopolymer films *vs* chloroform vapor pressure during solvent annealing.

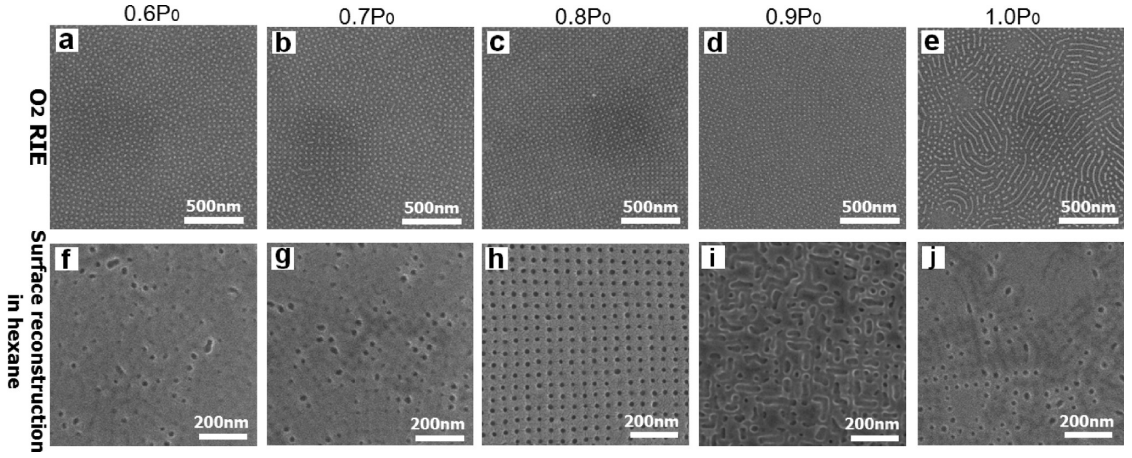

Figure 5. SEM images of PI-*b*-PS-*b*-PFS triblock terpolymer films annealed at (a, f) 0.6P_0, (b, g) 0.7P_0, (c, h) 0.8P_0, (d, i) 0.9P_0, and (e, j) 1.0P_0. The images in the top row show the morphologies after oxygen RIE, and the images in the bottom row show the morphologies after surface reconstruction in hexane. Annealing times are 1 h, except 30 min for 1.0P_0.

solvent vapor annealing system was used in which a stream of saturated chloroform vapor diluted by a carrier gas flowed into the chamber, Figure 4a. The design and operation of the flow-controlled solvent vapor annealing system will be discussed in detail elsewhere,[47] but briefly, nitrogen gas was bubbled through a liquid reservoir of chloroform at flow rates of 0−10 sccm and was diluted by a dry nitrogen gas flow of 0−10 sccm so that the total flow rate was 10 sccm into an annealing chamber of volume ~80 cm^3 containing the sample. The film thickness was measured by spectral reflectometry. The vapor pressure P of chloroform in the annealing chamber is given by

$$P = \frac{Q_{CHCl_3}}{Q_{CHCl_3} + Q_{N_2}} P_0$$

where Q_{CHCl_3} and Q_{N_2} are the flow rates of saturated chloroform vapor and nitrogen gas, respectively. P_0 is the saturated vapor pressure of chloroform, which is 205 Torr at the experimental temperature, 26 °C.

Figure 4b shows how the swelling behavior of the triblock terpolymer film varied with solvent vapor pressure during solvent annealing. The film annealed in saturated chloroform vapor pressure, 1.0P_0, dewetted after 30 min, but the swelling of the other samples at lower vapor pressures reached a stable value after about 40 min of annealing. The final swelling ratio (defined as swelled thickness/as-spun thickness) of those films increased with solvent vapor pressure. These data can be compared with the swelling ratios of the homopolymers at different vapor pressures, Figure 4c. The swelling ratio of homo-PS and homo-PFS films increased gradually with chloroform vapor pressure, but the swelling ratio of homo-PI increased more rapidly at higher vapor pressures. Chloroform is a good solvent for all three blocks, although its solubility parameter matches better with PS and PFS than with PI. The higher degree of swelling of PI is attributed to its high chain flexibility.[48] This suggests that the effective volume fraction of PI in the PI-*b*-PS-*b*-PFS triblock terpolymer film increased with chloroform vapor

pressure, which drives the changes of morphology described below.[49,50]

The SEM images in Figure 5 show morphologies of triblock terpolymer films after 1 h solvent annealing (or 30 min for the sample annealed at $1.0P_0$). The images in the top panels show the morphologies after oxygen RIE, and the images in the bottom panels the morphologies after surface reconstruction in hexane. At an intermediate vapor pressure, $0.8P_0$, a highly ordered square array of posts or holes was produced, as shown in Figure 5c,h, indicating that both PI and PFS produced cylindrical microdomains consistent with the schematic of Figure 1a. At a lower vapor pressure, $0.6P_0$ and $0.7P_0$, a square array of PFS posts was revealed after oxygen RIE, but the quality of ordering was poor compared to the result at $0.8P_0$. This is attributed to the lower chain mobility resulting from the lesser amount of solvent uptake by the film.[51] Moreover, surface reconstruction did not produce a square array of holes, which is consistent with lower swelling of PI, leading to spherical or elliptical microdomains that did not extend through the film thickness to the top surface, preventing reconstruction in hexane. Figure 5f,g shows that only a few of the PI microdomains intersected the surface. The presence of PI spheres in a square lattice was more clearly seen in the stained samples shown in Figure S1a and b. These SEM images confirmed that even though the PI microdomains were not opened by surface reconstruction, they were still present between the PFS microdomains. A few unopened holes were also seen in Figure 5h annealed at $0.8P_0$.

Figure 5d,i shows the morphology of the film annealed at a higher vapor pressure, $0.9P_0$. A square array of PFS posts was observed after oxygen RIE, but the morphology after surface reconstruction was a trench-like structure. The increased volume fraction of PI under high solvent vapor pressure conditions led to interconnection between the PI cylinders. Figure S1c shows the morphology of the stained sample. Finally, the morphology of the film annealed in saturated chloroform vapor, $1.0P_0$, is shown in Figure.5 e,j after 30 min of solvent annealing. Dewetting in some regions was accompanied by film thickening in the imaged regions, leading to in-plane cylinder morphologies as reported earlier.[30,31]

CONCLUSION

In summary, square-symmetry microdomains in films of a PI-*b*-PS-*b*-PFS triblock terpolymer can be processed to form two different patterns: a square array of posts using oxygen RIE or a square array of holes using surface reconstruction in hexane. The hole array can be transformed to a post array using oxygen RIE, and both patterns can be produced on a substrate. Pattern transfer into silicon substrates was demonstrated *via* dry and wet etching processes using the hole and post arrays as etching masks. The effect of solvent vapor pressure on the morphologies of the films was understood as a result of preferential swelling of the PI by chloroform. These results illustrate that the advantages of using a triblock terpolymer compared to a diblock copolymer for lithography are not only the wider range of morphologies available but also multiple routes for pattern development facilitated by the different chemical properties of each block.

EXPERIMENTAL METHODS

Substrate Preparation, Thin Film Deposition. Si(100) substrates with a native oxide layer were used. A P2VP brush layer was applied to promote perpendicular orientation of the cylindrical microdomains in the PI-*b*-PS-*b*-PFS triblock terpolymer film.[30] A 1% hydroxyl-terminated P2VP (M_n = 6.2 kg/mol, Polymer Source Inc.) solution in toluene was spin-coated on the silicon substrate and annealed at 170 °C overnight under vacuum. The ungrafted polymer was removed by rinsing in toluene. PI-*b*-PS-*b*-PFS (M_n = 82 kg/mol) with volume fractions of 25%, 65%, and 10% was synthesized as described in ref 31. A 0.85 wt % solution of the triblock terpolymer was blended with 0.15% of PS homopolymer solution (M_n = 27 kg/mol, Polymer Source Inc.) in toluene. This polymer blend solution was spin-coated on prepared P2VP-brushed silicon substrates to produce a film thickness of approximately 32 nm. In order to measure swelling of homopolymers, PI (M_n = 153 kg/mol, Polymer Source Inc.), PS (M_n = 500 kg/mol, Polymer Source Inc.), and PFS (M_n = 490 kg/mol, Polymer Source Inc.) homopolymer solutions in toluene were spin-coated onto silicon substrates.

Solvent Vapor Annealing. In the flow-controlled solvent annealing system, a saturated chloroform vapor was produced by bubbling nitrogen through liquid chloroform. The flow rates of the chloroform/nitrogen and pure nitrogen were regulated by mass flow controllers (MKS Inc., M100B) maintaining 10 sccm total flow. The partial pressure of chloroform in the annealing chamber of volume ~80 cm^3 was controlled by changing the ratio of the two gas streams. For example, the $0.8P_0$ condition was obtained by flowing 8 sccm of saturated chloroform vapor and 2 sccm of pure nitrogen gas. Triblock terpolymer films were annealed for 1 h except for the film treated at $1.0P_0$, which was annealed for 30 min.

Pattern Development and Transfer. To obtain a square array of posts, the annealed triblock terpolymer film was treated with RIE (30 s O_2, 6 mTorr, 90 W, Plasma Therm 790) to remove PS and PI and reveal oxidized PFS posts. To obtain a square array of holes, the film was immersed in hexane for 15 s and quenched with a nitrogen gun. To obtain hole and post mixed morphology, a TEM grid with holey carbon film (diameter of holes 1.2 μm, Ted Pella Inc.) was placed on top of a film with a hole array as a shadow mask, and reactive ion etching was performed through the holes of the shadow mask (30 s O_2, 6 mTorr, 90 W). A square array of silicon posts was formed from the PFS posts by CF_4 RIE (1 min, 10 mTorr, 50 W), and residual PFS was removed by O_2 RIE (1 min, 6 mTorr, 90 W). A square array of silicon pits was formed using the hole pattern as an etching mask. O_2 RIE (5 s, 10 mTorr, 90 W), CF_4 RIE (1 min, 10 mTorr, 50 W), and O_2 RIE (1 min, 6 mTorr, 90 W) were applied in sequence to remove the polymer brush layer at the bottom of the holes, etch the silicon wafer through the mask, and remove the residual polymer mask, respectively. A square array of silicon inverted pyramids was formed by transferring the hole pattern *via* anisotropic wet etching. First, holes in a triblock terpolymer were widened by O_2 RIE (15 s, 10 mTorr, 90 W; shown in Figure 2c). Then the silicon wafer was

etched through the widened holes in 30% KOH aqueous solution at room temperature and rinsed with water. The residual polymer mask was removed by O_2 RIE (1 min, 6 mTorr, 90 W).

Characterization. The surface morphologies of triblock terpolymer films and transferred silicon patterns were observed using SEM (Helios NanoLab 600, FEI; Gemini 982, Zeiss/Leo). Thin films of polymer samples were coated with a thin Au–Pd alloy in order to reduce charging effects. To increase the etch resistance of PI against O_2 RIE, triblock terpolymer films were stained by placing the samples in a chamber filled with OsO_4 vapor for 4 h. A spectral reflectometer (Filmetrics, Inc. F20-UV) was used for *in situ* film thickness measurments during annealing.

Conflict of Interest: The authors declare no competing financial interest.

Acknowledgment. This work was supported by the National Science Foundation, the Semiconductor Research Corporation, the Center on Functional Engineered and Nano Architectonics, Taiwan Semiconductor Manufacturing Company, and Tokyo Electron. H.K.C. acknowledges support from a National Research Foundation of Korea grant funded by the Korean Government (Ministry of Education, Science and Technology) [NRF-2010-357-D00075].

Supporting Information Available: Stained SEM images. This material is available free of charge *via* the Internet at http://pubs.acs.org.

REFERENCES AND NOTES

1. Park, M.; Harrison, C.; Chaikin, P. M.; Register, R. A.; Adamson, D. H. Block Copolymer Lithography: Periodic Arrays of 10^{11} Holes in 1 Square Centimeter. *Science* **1997**, *276*, 1401–1404.
2. Darling, S. B. Directing the Self-assembly of Block Copolymers. *Prog. Polym. Sci.* **2007**, *32*, 1152–1204.
3. Segalman, R. A. Patterning with Block Copolymer Thin Films. *Mater. Sci. Eng., R* **2005**, *48*, 191–226.
4. Park, C.; Yoon, J.; Thomas, E. L. Enabling Nanotechnology with Self Assembled Block Copolymer Patterns. *Polymer* **2003**, *44*, 6725–6760.
5. Kim, S. O.; Solak, H. H.; Stoykovich, M. P.; Ferrier, N. J.; de Pablo, J. J.; Nealey, P. F. Epitaxial Self-Assembly of Block Copolymers on Lithographically Defined Nanopatterned Substrates. *Nature* **2003**, *424*, 411–414.
6. Lazzari, M.; López-Quintela, M. A. Block Copolymers as a Tool for Nanomaterial Fabrication. *Adv. Mater.* **2003**, *15*, 1583–1594.
7. Bang, J.; Jeong, U.; Ryu, D. Y.; Russell, T. P.; Hawker, C. J. Block Copolymer Nanolithography: Translation of Molecular Level Control to Nanoscale Patterns. *Adv. Mater.* **2009**, *21*, 4769–4792.
8. Cheng, J. Y.; Ross, C. A.; Smith, H. I.; Thomas, E. L. Templated Self-Assembly of Block Copolymers: Top-Down Helps Bottom-Up. *Adv. Mater.* **2006**, *18*, 2505–2521.
9. Bita, I.; Yang, J. K. W.; Jung, Y. S.; Ross, C. A.; Thomas, E. L.; Berggren, K. K. Graphoepitaxy of Self-Assembled Block Copolymers on Two-Dimensional Periodic Patterned Templates. *Science* **2008**, *321*, 939–943.
10. Zheng, W.; Wang, Z.-G. Morphology of ABC Triblock Copolymers. *Macromolecules* **1995**, *28*, 7215–7223.
11. Bates, F. S.; Fredrickson, G. H. Block Copolymers—Designer Soft Materials. *Phys. Today* **1999**, *52*, 32–38.
12. Hadjichristidis, N.; Iatrou, H.; Pitsikalis, M.; Pispas, S.; Avgeropoulos, A. Linear and Non-Linear Triblock Terpolymers. Synthesis, Self-assembly in Selective Solvents and in Bulk. *Prog. Polym. Sci.* **2005**, *30*, 725–782.
13. Nagpal, U.; Detcheverry, F. A.; Nealey, P. F.; de Pablo, J. J. Morphologies of Linear Triblock Copolymers from Monte Carlo Simulations. *Macromolecules* **2011**, *44*, 5490–5497.
14. Han, W.; Tang, P.; Li, X.; Qiu, F.; Zhang, H.; Yang, Y. Self-Assembly of Star ABC Triblock Copolymer Thin Films: Self-Consistent Field Theory. *J. Phys. Chem. B* **2008**, *112*, 13738–13748.
15. Ludwigs, S.; Krausch, G.; Magerle, R.; Zvelindovsky, A. V.; Sevink, G. J. A. Phase Behavior of ABC Triblock Terpolymers in Thin Films: Mesoscale Simulations. *Macromolecules* **2005**, *38*, 1859–1867.
16. Feng, J.; Ruckenstein, E. Monte Carlo Simulation of Triblock Copolymer Thin Films. *Polymer* **2002**, *43*, 5775–5790.
17. Mogi, Y.; Kotsuji, H.; Kaneko, Y.; Mori, K.; Matsushita, Y.; Noda, I. Preparation and Morphology of Triblock Copolymers of the ABC Type. *Macromolecules* **1992**, *25*, 5408–5411.
18. Stadler, R.; Auschra, C.; Beckmann, J.; Krappe, U.; Voigt-Martin, I.; Leibler, L. Morphology and Thermodynamics of Symmetric Poly (A-block-B-block-C) Triblock Copolymers. *Macromolecules* **1995**, *28*, 3080–3097.
19. Breiner, U.; Krappe, U.; Thomas, E. L.; Stadler, R. Structural Characterization of the "Knitting Pattern" in Polystyrene-block-poly(ethylene-co-butylene)-block-poly(methyl Methacrylate) Triblock Copolymers. *Macromolecules* **1998**, *31*, 135–141.
20. Bohbot-Raviv, Y.; Wang, Z.-G. Discovering New Ordered Phases of Block Copolymers. *Phys. Rev. Lett.* **2000**, *85*, 3428–3431.
21. Chuang, V. P.; Ross, C. A.; Gwyther, J.; Manners, I. Self-Assembled Nanoscale Ring Arrays from a Polystyrene-b-polyferrocenylsilane-b-poly(2-vinylpyridine)Triblock Terpolymer Thin Film. *Adv. Mater.* **2009**, *21*, 3789–3793.
22. Dupont, J.; Liu, G. ABC Triblock Copolymer Hamburger-like Micelles, Segmented Cylinders, and Janus Particles. *Soft Matter* **2010**, *6*, 3654–3661.
23. Wang, C.; Lee, D. H.; Hexemer, A.; Kim, M. I.; Zhao, W.; Hasegawa, H.; Ade, H.; Russell, T. P. Defining the Nanostructured Morphology of Triblock Copolymers Using Resonant Soft X-ray Scattering. *Nano Lett.* **2011**, *11*, 3906–3911.
24. Phillip, W. A; Dorin, R. M.; Werner, J.; Hoek, E. M. V.; Wiesner, U.; Elimelech, M. Tuning Structure and Properties of Graded Triblock Terpolymer-Based Mesoporous and Hybrid Films. *Nano Lett.* **2011**, *11*, 2892–2900.
25. Lee, D. H.; Park, S.; Gu, W.; Russell, T. P. Highly Ordered Nanoporous Template from Triblock Copolymer. *ACS Nano* **2011**, *5*, 1207–1214.
26. Matsen, M. W.; Bates, F. S. Unifying Weak- and Strong-Segregation Block Copolymer Theories. *Macromolecules* **1996**, *29*, 1091–1098.
27. Khandpur, A. K.; Förster, S.; Bates, F. S.; Hamley, I. W.; Ryan, A. J.; Bras, W.; Almdal, K.; Mortensen, K. Polyisoprene-polystyrene Diblock Copolymer Phase Diagram Near the Order-Disorder Transition. *Macromolecules* **1995**, *28*, 8796–8806.
28. Matsen, M. W.; Bates, F. S. Block Copolymer Microstructures in the Intermediate-Segregation Regime. *J. Chem. Phys.* **1997**, *106*, 2436–2448.
29. Tang, C.; Bang, J.; Stein, G. E.; Fredrickson, G. H.; Hawker, C. J.; Kramer, E. J.; Sprung, M.; Wang, J. Square Packing and Structural Arrangement of ABC Triblock Copolymer Spheres in Thin Films. *Macromolecules* **2008**, *41*, 4328–4339.
30. Son, J. G.; Gwyther, J.; Chang, J.-B.; Berggren, K. K.; Manners, I.; Ross, C. A. Highly Ordered Square Arrays from a Templated ABC Triblock Terpolymer. *Nano Lett.* **2011**, *11*, 2849–2855.
31. Chuang, V. P.; Gwyther, J.; Mickiewicz, R. A.; Manners, I.; Ross, C. A. Templated Self-Assembly of Square Symmetry Arrays from an ABC Triblock Terpolymer. *Nano Lett.* **2009**, *9*, 4364–4369.
32. Mogi, Y.; Nomura, M.; Kotsuji, H.; Ohnishi, K.; Matsushita, Y.; Noda, I. Superlattice Structures in Morphologies of the ABC Triblock Copolymers. *Macromolecules* **1994**, *27*, 6755–6760.
33. Tang, C.; Lennon, E. M.; Fredrickson, G. H.; Kramer, E. J.; Hawker, C. J. Evolution of Block Copolymer Lithography to Highly Ordered Square Arrays. *Science* **2008**, *322*, 429–432.
34. Park, S.-M.; Craig, G. S. W.; La, Y.-H.; Solak, H. H.; Nealey, P. F. Square Arrays of Vertical Cylinders of PS-b-PMMA on Chemically Nanopatterned Surfaces. *Macromolecules* **2007**, *40*, 5084–5094.
35. Hur, S.-M.; García-Cervera, C. J.; Kramer, E. J.; Fredrickson, G. H. SCFT Simulations of Thin Film Blends of Block

Copolymer and Homopolymer Laterally Confined in a Square Well. *Macromolecules* **2009**, *42*, 5861–5872.
36. Bang, J.; Kim, S. H.; Drockenmuller, E.; Minsner, M. J.; Russell, T. P.; Hawker, C. J. Defect-Free Nanoporous Thin Films from ABC Triblock Copolymers. *J. Am. Chem. Soc.* **2006**, *128*, 7622–7629.
37. Elbs, H.; Fukunaga, K.; Stadler, R.; Sauer, G.; Magerle, R.; Krausch, G. Microdomain Morphology of Thin ABC Triblock Copolymer Films. *Macromolecules* **1999**, *32*, 1204–1211.
38. Luo, C.; Huang, W.; Han, Y. Order-Order Transition of C → sdG → sL → S in ABC Triblock Copolymer Thin Film Induced by Solvent Vapor. *Macromol. Rapid Commun.* **2009**, *30*, 515–520.
39. Guo, S.; Rzayev, J.; Bailey, T. S.; Zalusky, A. S.; Olayo-Valles, R.; Hillmyer, M. A. Nanopore and Nanobushing Arrays from ABC Triblock Thin Films Containing Two Etchable Blocks. *Chem. Mater.* **2006**, *18*, 1719–1721.
40. Tang, C.; Sivanandan, K.; Stahl, B. C.; Fredrickson, G. H.; Kramer, E. J.; Hawker, C. J. Multiple Nanoscale Templates by Orthogonal Degradation of a Supramolecular Block Copolymer Lithographic System. *ACS Nano* **2010**, *4*, 285–291.
41. Xu, T.; Stevens, J.; Villa, J. A.; Goldbach, J. T.; Guarini, K. W.; Black, C. T.; Hawker, C. J.; Russell, T. P. Block Copolymer Surface Reconstuction: A Reversible Route to Nanoporous Films. *Adv. Funct. Mater.* **2003**, *13*, 698–702.
42. Park, S.; Kim, B.; Wang, J.-Y.; Russell, T. P. Fabrication of Highly Ordered Silicon Oxide Dots and Stripes from Block Copolymer Thin Films. *Adv. Mater.* **2008**, *20*, 681–685.
43. Tabata, O.; Asahi, R.; Funabashi, H.; Shimaoka, K.; Sugiyama, S. Anisotropic Etching of Silicon in TMAH Solutions. *Sens. Actuators, A* **1992**, *34*, 51–57.
44. Hantschel, T.; Vandervorst, W. Anisotropic Etching of Inverted Pyramids in the Sub-100 nm Region. *Microelectron. Eng.* **1997**, *35*, 405–407.
45. Lee, J. Y.; Sun, K.; Li, B.; Xie, Y.-H.; Wei, X.; Russell, T. P. Multiple-Level Threshold Switching Behavior of In_2Se_3 Confined in a Nanostructured Silicon Substrate. *Appl. Phys. Lett.* **2010**, *97*, 092114.
46. Giermann, A. L.; Thompson, C. V. Solid-State Dewetting for Ordered Arrays of Crystallographically Oriented Metal Particles. *Appl. Phys. Lett.* **2005**, *86*, 121903.
47. Gotrik, K.; Hannon, A.; Son, J. G.; Keller, B.; Alexander-Katz, A.; Ross, C. A. Morphology Control in Block Copolymer Films using Mixed Solvent Vapors. *ACS Nano*, published online August 28, 2012, doi: 10.1021/nn302641z.
48. Bahadur, P.; Sastry, N. V. *Principles of Polymer Science*, 2nd ed.; Alpha Science International Ltd., 2005; pp 162−166.
49. Bosworth, J. K.; Paik, M. Y.; Ruiz, R.; Schwartz, E. L.; Huang, J. Q.; Ko, A. W.; Smilgies, D.-M.; Black, C. T.; Ober, C. K. Control of Self-Assembly of Lithographically Patternable Block Copolymer Films. *ACS Nano* **2008**, *2*, 1396–1402.
50. Jung, Y. S.; Ross, C. A. Solvent-Vapor-Induced Tunability of Self-Assembled Block Copolymer Patterns. *Adv. Mater.* **2009**, *21*, 2540–2545.
51. Jung, Y. S.; Chang, J.-B.; Verploegen, E.; Berggren, K. K.; Ross, C. A. A Path to Ultranarrow Patterns Using Self-Assembled Lithography. *Nano Lett.* **2010**, *10*, 1000–1005.